

Radar Echo Population of Air-Mass Thunderstorms and Nowcasting of Thunderstorm-Induced Local Heavy Rainfalls Part II: A Feasibility Study on Nowcasting

Masahito Ishihara

Educational Unit for Adaptation to Extreme Weather Conditions and Resilient Society,
Center for the Promotion of Interdisciplinary Education and Research, Kyoto University
Gokasho, Uji, Kyoto 611-0011, Japan
E-mail: ishihara.masahito.7u@kyoto-u.ac.jp

Many air-mass thunderstorms were generated in the Tokyo metropolitan area on August 5, 2008, when a severe local rainstorm caused a flash flood in the center of Tokyo. Using three-dimensional radar reflectivity data from the Japan Meteorological Agency (JMA), nowcasting was examined concerning the peak time and peak rainfall intensity of thunderstorms. Four qualitative forecast methods – precipitation cores aloft, time changes in vertically integrated liquid water, time changes in echo-top height, lightning activity – and three quantitative forecast methods using three parameters were adopted in eight thunderstorms related to heavy-rainfall warnings issued by the JMA on August 5, 2008. While there is much worth further examination in the method using precipitation core aloft, the other methods are not in the stage of operational use in order to forecast time and rainfall intensity at the rainfall peak of each thunderstorm.

Keywords: thunderstorm, local heavy rainfall, weather radar, statistics, nowcasting

1. Introduction

Using three-dimensional radar data from the Japan Meteorological Agency (JMA), Ishihara (2013) [1] made statistical research and presented a comprehensive understanding of the morphology of 179 air-mass thunderstorms generated in and around Tokyo on August 5, 2008, when heavy local rainfall occurred in Zoshigaya, Tokyo. One third of all of these thunderstorms had a diameter of 3.5 km or less, and the mean diameter was 5.5 km; they were thus small, in general. The mode (the value that appears most often in a set of data) of their lifetime was between 20 and 40 minutes, and 86% of all existed for less than 80 minutes. The elapse times from when a thunderstorm was recognized as a convective cell (defined later) using radars until rainfall on the surface peaked were 10 to 30 minutes in almost all cases. It should be noted that these results were obtained from distribution of rain-

drops, thus being less than those from visible observation. While the rainfall amount caused by each thunderstorm was less than 40 mm in half of the total of thunderstorms, one third of the total of thunderstorms brought about rainfall amounts of greater than 60 mm. This fact supports the existence of difficulty in monitoring and forecasting of heavy local rainfall caused by air-mass thunderstorms that is called “unstable rainfall” by weather-forecasters in Japan [2].

Nowcasting of rainfall is one of the most urgent issues among the national meteorological and hydrological services of the world, and various nowcasting systems have been developed and operated. Examples are “the precipitation nowcast” and “the short-term precipitation forecast” of the JMA [3, 4], WDSS (Warning Decision Support System)-II of the National Weather services of the United States [5], TITAN (Thunderstorm Identification Tracking Analysis and Nowcasting) of NCAR of the United States [6], Nimrod (Automated precipitation nowcasting system utilizing rainfall radar data) [7] and Generating Advanced Nowcasts for Deployment in Operational Land-based Flood forecasts (GAN-DORF) [8] of the Met Office of the United Kingdom, CARDS (Canadian Radar Decision Support System) [9] of the Weather office of Canada, and NinJo of Deutscher Wetterdienst [10]. Comparison experiments were conducted for some of these methods as part of a forecasting demonstration by the WMO at the Sydney (2000) and Beijing (2008) Olympics [11, 12, 13]. Because these nowcasting systems basically use real-time radar data as initial values and temporal extrapolation methods [11], they are not capable, however, of responding to processes such as generation, rapid development/decline, merging, and organization of thunderstorms.

In order to understand the vertical evolution of thunderstorms by means of radar observation, three-dimensional rainfall distribution should be used rather than traditional two-dimensional radar data. The JMA radar operation system started to provide nationwide radar reflectivity factor data on 1 km meshes in horizontal and vertical (hereafter, 3-D radar data) every 10 minutes in accordance with an update of the system in 2005 [14]. From then, the

1. This paper is translated with revision from the TENKI journal published by the Meteorological Society of Japan.

JMA has technically strengthened the system's ability for monitoring and forecasting heavy rainfall using 3-D radar data [15].

In this paper, using mainly 3-D radar data the possibility of very short-term forecasting of the time of rainfall peak and its intensity with a lead time (time from issuing forecast to start of heavy rainfall) of several 10 minutes will be discussed targeting thunderstorms generated in the Tokyo metropolitan area on August 5, 2008. This is termed "nowcasting of rainfall" in this study.

A convective precipitation area whose radar reflectivity factor (hereafter "reflectivity") at the 2 km level (Z_{2km}) reaches 35 dBZ or more during its lifetime with one reflectivity peak is regarded as a "convective cell." The JMA defines heavy rainfall as "rain that might cause a disaster" [16]. Warnings issued by the JMA are defined as "forecasts alerting to the possibility of a disaster when it might occur."

2. Data

Radar data are first obtained on polar coordinates with multiple elevation-angle PPI obtained from 20 radar sites in Japan with a resolution of 500 m in range and 0.7 degree in azimuthal direction. Nationwide 3-D radar data are then produced with conversion from polar coordinate to Cartesian coordinates spaced at 0.50 minutes latitude (nearly 1 km), 0.75 minutes longitude (nearly 1 km), and 1 km in height. Simple linear interpolation is used to make data in the vertical. Reflectivity data for 15 layers and vertically integrated liquid water (hereafter "VIL") data are used in this research. Rain water amount M for 15 individual layers is calculated from reflectivity Z as $M = 3.44 \times 10^{-3} Z^{4.7}$ [17] (the unit for M is gm^{-3} , that for Z is mm^6m^{-3}), and VIL is determined by integrating M for 15 layers in the vertical. The unit for VIL used in this paper is kgm^{-2} .

3. Analysis Methods

One of the important issues in weather-forecast operations is to provide heavy rainfall or flood warnings associated with thunderstorms as soon as possible without increasing the false-alert rate [2]. The following are subjects in the nowcasting of rainfall associated with thunderstorms:

- (1) Location and time of thunderstorm occurrence,
- (2) Peak time of rainfall caused by thunderstorms,
- (3) Rainfall intensity at the rainfall peak,
- (4) Moving vector of thunderstorms,
- (5) Lifetime of thunderstorms (forecast of dissipation time),
- (6) Total rainfall amount caused by thunderstorms,
- (7) Development due to multicellular processes, merging of thunderstorms and organization into mesoscale convective systems.

This paper will discuss the nowcasting of rainfall associated with thunderstorms and the issuing of heavy rainfall warnings focusing on subjects (2) and (3), above. A nowcasting method using GPS precipitable water [18] is proposed for (1). Real-time analysis of a very high-density surface network might be useful for (1). A method for (4) has already been operated in the precipitation nowcasting of the JMA [4]. A cloud-resolving numerical model with real-time data assimilation of various observation data would be one of the final solutions for (5)-(7). Subjects (1) and (5)-(7) remain as issues to be discussed in the future.

4. Nowcasting of Rainfall Peak

4.1. Selection of Convective Cells

The targets of this study are eight convective cells generated in areas C to F in Fig. 1: C1, C3, D1, D2, D3, E1, E2, F1. They had one-hour rainfall amounts of 47 mm or larger except for D3, and heavy rainfall warnings were issued by the JMA in these areas on August, 2008. These convective cells are here termed "heavy rainfall convective cells." Two convective cells with a rainfall amount of less than 50 mm per hour – S1 and S2 – are chosen as comparison cases and termed "nonheavy rainfall convective cells."

In order to know the status of these 10 convective cells in the group of 179 convective cells generated in the Tokyo metropolitan area on August 5, 2008 (Ishihara 2013), cumulative frequency distribution concerning the maximum area and lifetime of individual convective cells is shown in Fig. 2. Seven heavy rainfall convective cells excluding F1 had a larger area than the 2 nonheavy rainfall convective cells (S1, S2) (Fig. 2a), and were relatively large convective cells with a cumulative frequency of area of greater than 80% in the group of 179 convective cells. Lifetimes of all convective cells range from 60 to 160 minutes, and there is no systematic difference between heavy and nonheavy rainfall convective cells (Fig. 2b).

Figure 3 shows time changes in the echo distribution of convective cells C1 to E2 every 20 minutes, and Fig. 4 indicates their schematic diagrams. C1 was generated in the southern part of Central Tokyo at 1120 Japan Standard Time (JST) and grew to a larger convective cell by 1200 JST, merging with C2 generated north of C1. C1 caused local heavy rainfall around 1200 JST when it reached Zoshigaya, Tokyo. C3 was generated close to C1 at 1150 JST. C1 and C3 seemed to be formed together as a multicell convection system. D1 was generated in the northern part of Kawasaki city at 1120 JST. D2 was generated only 4 km apart from D1 at 1300 JST, when D1 was at the decaying stage in its evolution. D3 was also generated nearby D2 at 1410 JST. D1, D2, and D3 seemed

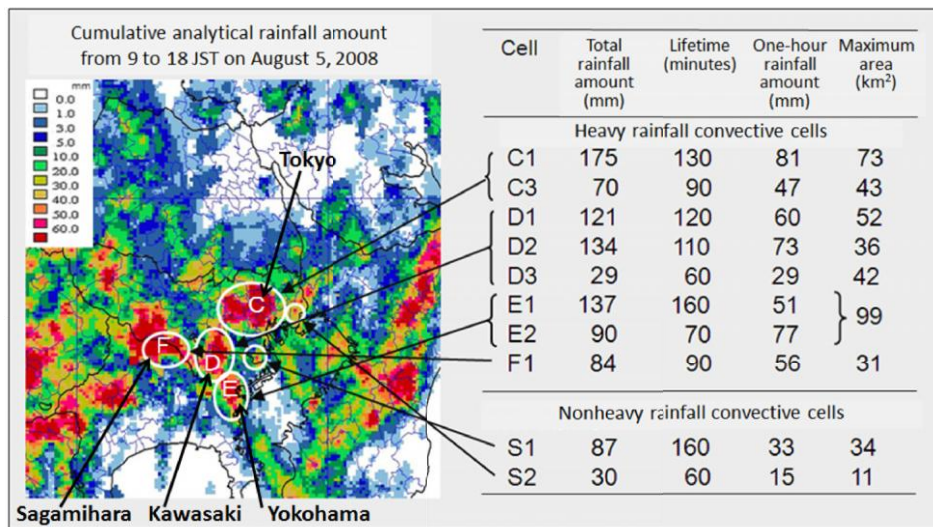


Fig. 1. Ten convective cells studied for rainfall peak nowcasting shown on a map for cumulative analytical rainfall amounts for the 9 hours from 0900 to 1800 JST on August 5, 2008. "Total rainfall amount" is an integrated value of the highest rainfall intensity value within each convective cell each 10 minutes, multiplied by 1/6 during generation to dissipation of convective cells. "One-hour rainfall amount" is the total rainfall amount divided by the lifetime (hour) of each convective cell. "Maximum area" is the maximum area of reflectivity at the 2 km level from generation to dissipation of each convective cell.

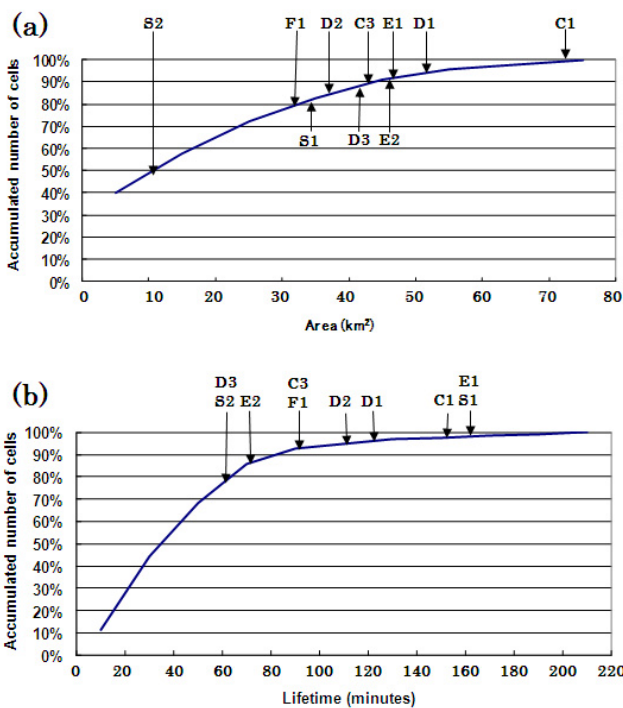


Fig. 2. Status of 10 convective cells in cumulative frequency distributions of area (a) and of lifetime (b) in the group of 179 convective cells.

to be forming a multicell convection system in all. E1 and E2 were separately generated in the eastern part of Yokohama city and then merged into a larger convective cell. F1 was solely generated in the southern part of South Tama, Tokyo and Sagami-hara city, Kanagawa. S1 and S2 in Fig. 1 are convective cells separately generated and maintained for longer and shorter periods, respectively.

Figure 4 shows times of the generation and dissipation of convective cells and issue times of JMA heavy-rainfall/flooding advisories (A) and heavy-rainfall/flooding warnings (W). Advisories were issued before the occurrence of the 8 heavy-rainfall convective cells. Warnings were, however, issued after the generation or dissipation of convective cells, and no warnings were issued before rainfall peaks in any case.

4.2. Forecasting Methods

The local maximum point of reflectivity on the 3-D coordinate grids inside a convective cell is defined as a "core." Heights of cores change with time. A time-height cross-section is made from vertical reflectivity profiles passing through each core. Rainfall intensity estimated from reflectivity at the 1 km level using empirical Z-R relational expression $Z = 200R^{1.6}$ (units for Z and R are mm^6m^{-3} and mmh^{-1} , respectively) [19, 20] is defined as rainfall intensity near the surface. The reason for using reflectivity-induced rainfall intensity values here, which are not calibrated by rain gauges, is to maintain consistency with VIL values that are also calculated from reflectivity values.

Forecasting of the appearance of rainfall peaks near the surface in each convective cell (hereafter "rainfall peak") is attempted using the following 7 methods:

- (1) Formation of the core aloft and descent toward the surface (hereafter "core aloft"),
- (2) Time change in maximum values of VIL in convective cells (abbreviated as VIL),
- (3) Time change in echo-top height using the reflectivity of 10 dBZ as the threshold,

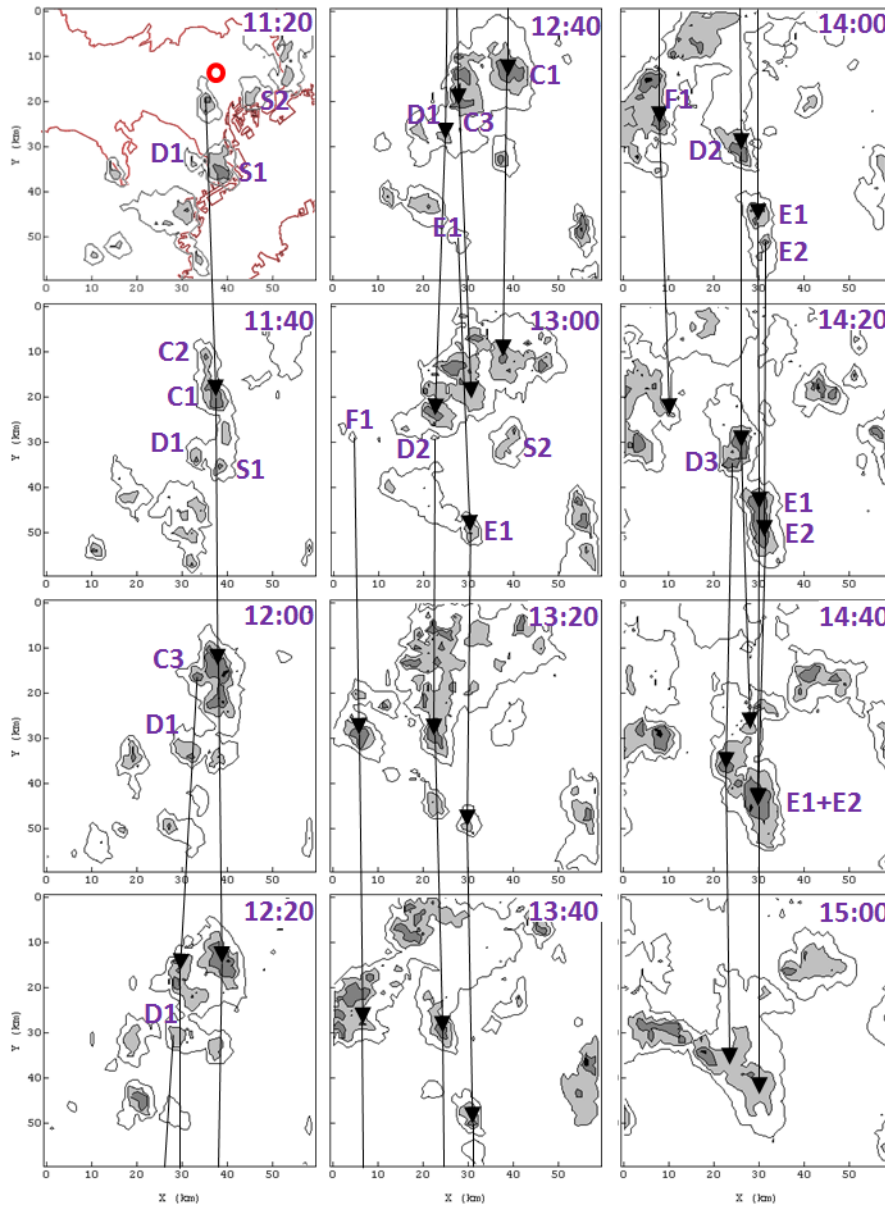


Fig. 3. Time changes in radar echoes of 10 convective cells every 20 minutes. Contours are reflectivity of 10, 35, 45, 55 dBZ at the 2 km level. Areas greater than 35 dBZ are shown in gray, greater than 45 dBZ in dark gray, and greater than 55 dBZ in black. The circle at 1120 JST shows the location of Zoshigaya, Tokyo.

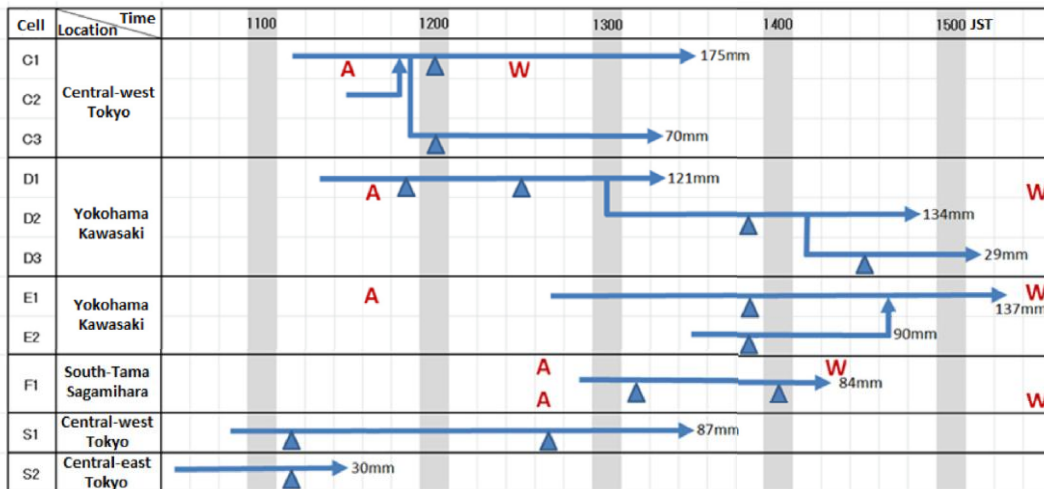


Fig. 4. Schematic diagrams of evolution of 10 convective cells. “A” indicates the time at which heavy rainfall and flooding advisories were issued by the JMA, “W” that of heavy rainfall and flooding warnings. Triangles show occurrence times of rainfall peaks, and figures next to arrows are integrated rainfall amounts estimated from radar data at the heaviest rainfall points of individual convective cells.

- (4) Lightning activity; cloud-to-ground lightning discharge (abbreviated as G) and lightning inside and within a 2-km region from convective cells (abbreviated as C), detected by the lightning detection system of JMA “LIDEN” [21] are examined. As shown in Fig. 6 of Takahashi (1984) [22], when snow crystals and graupel particles produced inside thunderstorms collide with each other in a layer colder (warmer) than -10° , they are charged positively and negatively (negatively and positively), respectively. They separate upward and downward due to differences in falling speed and the presence of updrafts, and then lightning occurs to cancel the resulting potential electricity difference. Graupel particles are produced only within strong updrafts, which may cause heavy rainfall on the surface. Taking these into account, lightning activity is considered as a forecasting factor in the initiation of heavy rainfall. LIDEN detects G using long electric waves and C using ultra-short electric waves. The 0° level was 4.9 km and that of -10° was 7.0 km according to upper-air sounding at Tateno (Tsukuba city) at 0900 JST on August 5, 2008.
- (5) Three methods for quantitatively forecasting rainfall intensity at a rainfall peak
- Continuation forecast; no change in rainfall intensity values until 10 minutes later is assumed. The JMA operated “precipitation nowcasting” and “short-term precipitation forecasting” based on this method, including some modulation of precipitation due to orography effects.
 - Extrapolation forecast; linear extrapolation is made using the change rate for the latest 10 minutes of rainfall intensity.
 - RadVil forecast; forecasting of rainfall intensity values is made using the rainfall forecasting model “RadVil” constructed by Boudevillain et al. (2006) [23]. The time change in VIL is the difference between the generated rain water amount in clouds and the vertical flux of rain water at the bottom of clouds (rainfall intensity). RadVil assumes that the generation rate of rain water in clouds and the vertical flux do not change during forecast time (10 minutes), and rainfall intensity 10 minutes later is forecasted from values of VIL and rainfall intensity. (See the appendix for further information.) The RadVil method differs from the methods a and b, because it apparently considers generation of rain water in clouds. In methods b and c, forecast values were obtained from 10 minutes after the start of observation of convective cells.

4.3. Nowcasting of Rainfall Peak

a. Convective cell C1

Figure 5 shows a time-height cross-section for convective cell C1. Time changes in rainfall intensity at the 1 km

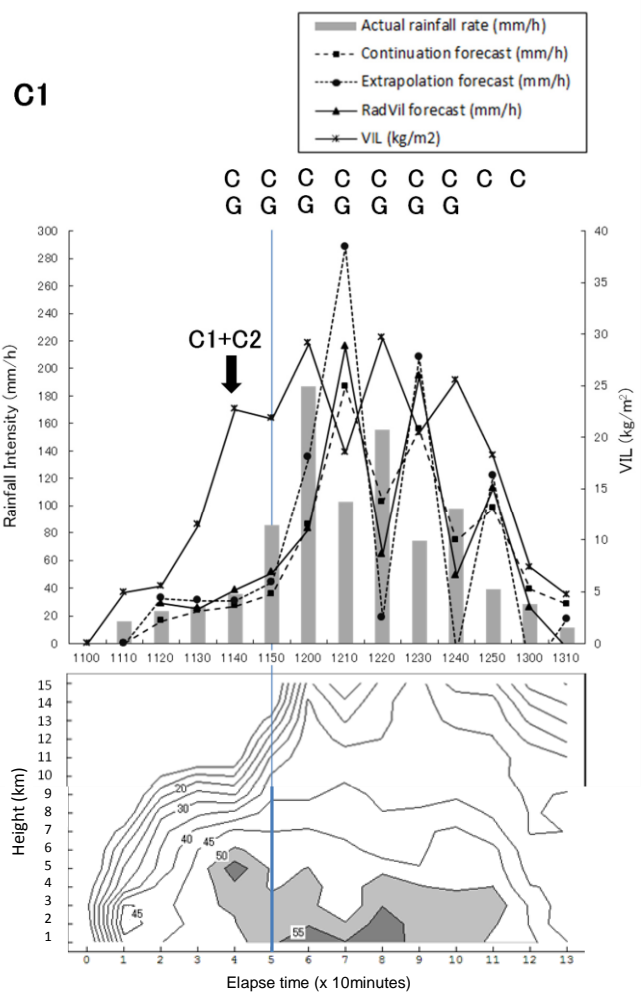


Fig. 5. Time-height cross-section of reflectivity (dBZ) passing through the precipitation core in convective cell C1 (bottom), rainfall intensity at the 1 km level (bar graph), vertically integrated liquid water (VIL, solid line), continuation forecast for rainfall intensity 10 minutes before each instance (broken line), extrapolation forecast (dotted line), and RadVil forecast by Boudevillain et al. (2006) [23] (thin solid line). A vertical line in the cross-section shows the generation time of peaks of rainfall on the surface. C shows intracloud lightning and G cloud-to-ground lightning detected by JMA LIDEN.

level, VIL, and 3 forecast values of rainfall intensity are also shown. The cross-section indicates the period from when radar echoes of the reflectivity of 10 dBZ appeared until they could not be identified as convective cells any more.

As described in Section 4.1, C1 was generated in the southern part of Central Tokyo at 1100 JST, slowly moved to the north and rapidly developed after merging with smaller convective cell C2 at 1150 JST. Rainfall peaked at 1200 JST (rainfall intensity of 187 mm/h), around which heavy local rainfall occurred at Zoshigaya [24,25,26]. At this time, a flash flood occurred at a sewer construction site located in the northwestern part of C1, causing an incident in which 5 workers were swept away and killed [27]. One reason why C1 caused particularly heavy

Table 1. Summary for nowcasting rainfall peaks of 10 convective cells using 4 qualitative forecasting methods and 3 quantitative forecasting methods. “n/a” indicates “not effective” or “not generated.” 1) and 2) refer to two rainfall peaks in a convective cell.

Convective cell	Total rainfall amount (mm)	Lifetime (minutes)	Generation and development status	Methods for forecasting surface rainfall peak				
				Core aloft	VIL (Vertically Integrated Liquid water)	Echo-top height	Lightning activity: In-cloud (C) Cloud to ground (G)	Continuation forecast Extrapolation forecast RadVil forecast
Heavy rainfall convective cells								
C1	175	130	Generated solely and merged with C2	Core of 58 dBZ at the 5 km level 20 minute before the rainfall peak	Rapidly increased and peaked 20 minutes before the rainfall peak	Rapidly increased 10-20 minutes before the rainfall peak	C and G from 10 minutes before the rainfall peak	3 methods forecasted the rapid increase of rainfall intensity until the rainfall peak in spite of smaller values than the actual.
C3	70	90	Generated at the west end of C1	n/a	n/a	n/a	C from 10 minutes before	n/a
D1	121	120	Generated solely with 2 rainfall peaks	1) Core of 51 dBZ at the 2 km level before 10 minutes 2) n/a	1) Peaked 10 minutes before 2) n/a	1) n/a 2) Rapidly increased 10-20 minutes before	1) C from 30 minutes before 2) C at the peak	1) Continuation and RadVil forecasts showed a false peak 10 minutes before the true peak. 2) n/a
D2	134	110	Generated at the south end of D1	Core of 50 dBZ at the 2-4 km levels 50 minutes before	Peaked 30 minutes before	n/a	C and G from 20 minutes before	3 methods underestimated the rainfall peak
D3	29	60	Generated at the south end of D2	Core of 54 dBZ at the 3 km level 10 minutes before	n/a	Rapidly increased 10-20 minutes before	n/a	RadVil forecasts was effective before the peak.
E1	137	160	Generated solely And merged with E2 with 2 rainfall peaks	Core of 54 dBZ at the 2 km level 10 minutes before	Increased from 20 minutes before	n/a	n/a	n/a
E2	90	70	Generated solely and merged with E1	Core of 53 dBZ at the 2 km level 10 minutes before	n/a	n/a	n/a	n/a
F1	84	90	Generated solely with 2 rainfall peaks	1) n/a 2) n/a	1) n/a 2) n/a	1) Rapidly increased 10-20 minutes before 2) n/a	1) n/a 2) C and G from 30 minutes before	1) n/a 2) Three forecasting methods were effective before the peak.
Nonheavy rainfall convective cells								
S1	87	160	Generated solely and disappeared with 3 convective cores	1) n/a 2) n/a	1) n/a 2) n/a	1) Rapidly increased 10-20 minutes before 2) n/a	1) n/a 2) G at 30 minutes before	1) n/a 2) n/a
S2	30	60	Generated solely and disappeared	Core of 46 dBZ at the 3 km level 10 minutes before	Peaked at 10 minutes before		n/a	Extrapolation and RadVil forecasts were effective before the peak.

rainfall is considered to be the merging with C2.

A core of 49 dBZ appeared at the 2 km level at 1110 JST in Fig. 5, changed its reflectivity to 42 dBZ at the 3 km level at 1120 JST, 49 dBZ at the 3 km level at 1130 JST, and finally reached the 5 km level with reflectivity of 58 dBZ at 1140 JST. The core turned to descending after 1140 JST and reached the 1 km level at 1200 JST, when surface rainfall peaked. The descending speed of the core aloft between 1140 and 1200 JST was 3.3 ms^{-1} . If weather forecasters had paid attention to the behavior of this core, it could have been able to forecast the beginning of heavy rainfall 20 minutes before the rainfall peak. We hereafter define a “rainfall peak” at which rainfall intensity increased about 40 mm/h during 20 minutes and decreased after that.

VIL varied with almost the same phase as the time-change of rainfall intensity during the whole period, but it increased rapidly from 12 to 22 kgm^{-2} during the 10 minutes from 1130 to 1140 JST before the rainfall peak. The rapid increase of VIL seemed to correspond to the creation of the core aloft and also to the advent of the rainfall peak.

Echo-top height (contours of 10 dBZ in Fig. 5) was nearly constant at 10 km from 1120 to 1140 JST and in-

creased to 13 km at 1150 JST, indicating the rapid vertical development of convection at that time. C and G lightning was detected from 10 minutes before the rainfall peak and hinted at the occurrence of the rainfall peak.

Quantitative forecasting of rainfall intensity is discussed here. Note that, for example, the forecast values at 1200 JST in Fig. 5 were obtained at 1150 JST. Rainfall intensity values forecasted by the three methods showed a rapid increase in rainfall intensity until the rainfall peak at 1200 JST. They were, however, smaller than the actual value (the value determined by radar observation). After the rainfall peak, extrapolation values and RadVil values showed unrealistically large values. In other words, these methods are not available after the rainfall peak. Although RadVil had been expected to show better forecasting effect than continuation and extrapolation methods as suggested by Boudevillain et al. (2006) [23], there were no differences among them in forecast accuracy.

b. Other convective cells

Figures 6 to 14 show the status for 9 convective cells other than C1. A brief overview is given here, and analysis results for each convective cell are summarized in Table 1.

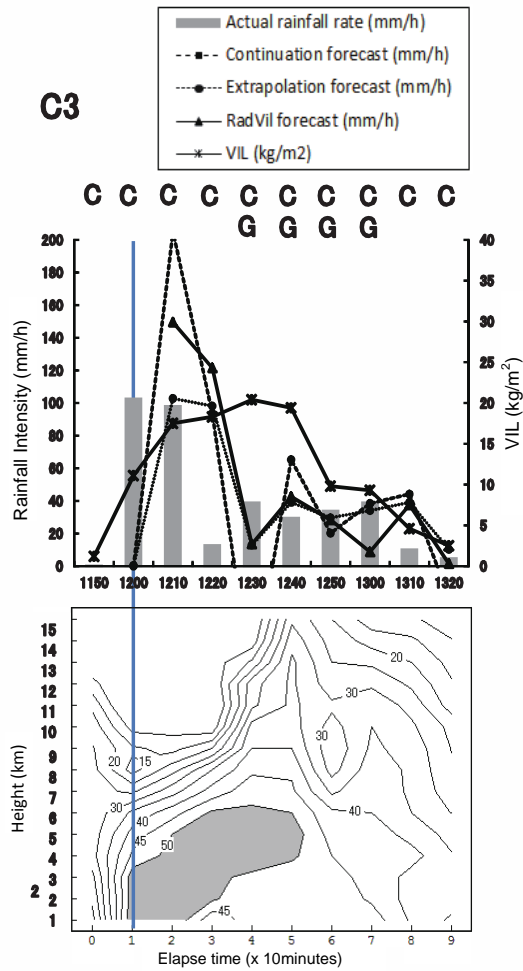


Fig. 6. Same as Fig. 5 for convective cell C3.

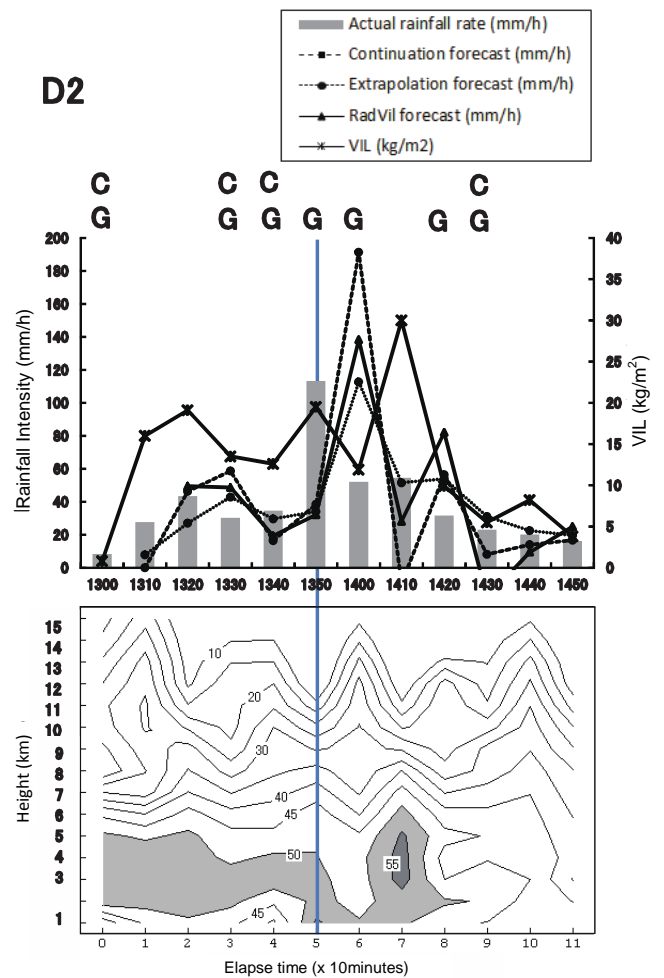


Fig. 8. Same as Fig. 5 for convective cell D2.

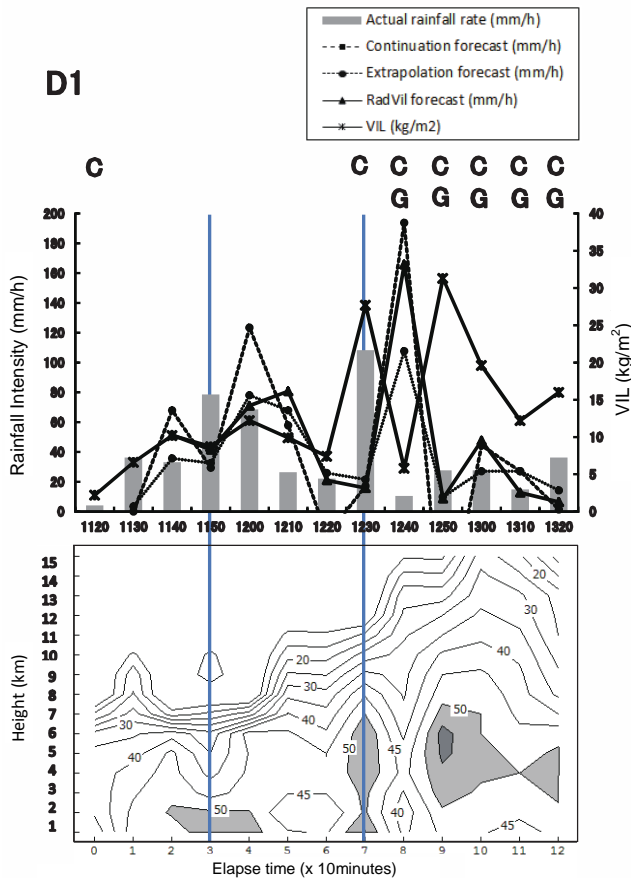


Fig. 7. Same as Fig. 5 for convective cell D1.

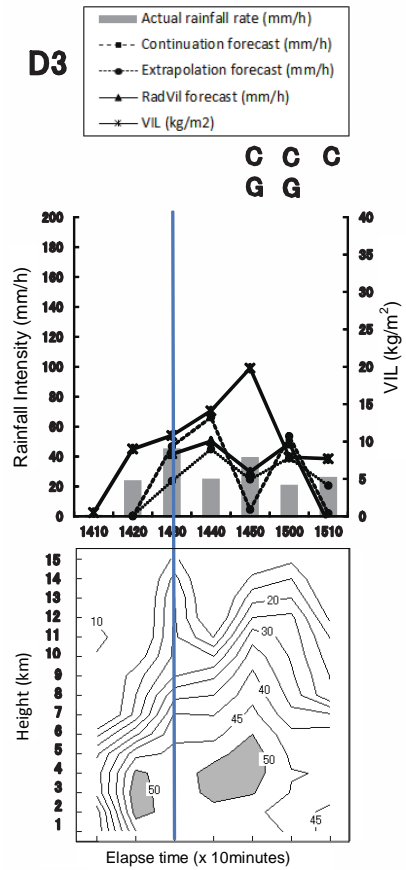


Fig. 9. Same as Fig. 5 for convective cell D3.

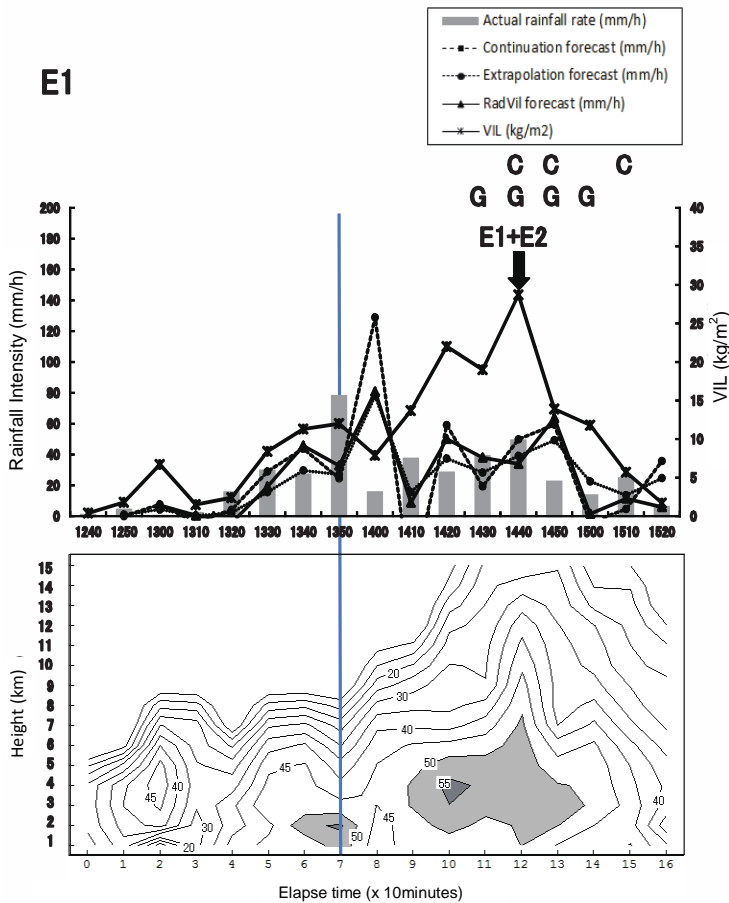


Fig. 10. Same as Fig. 5 for convective cell E1.

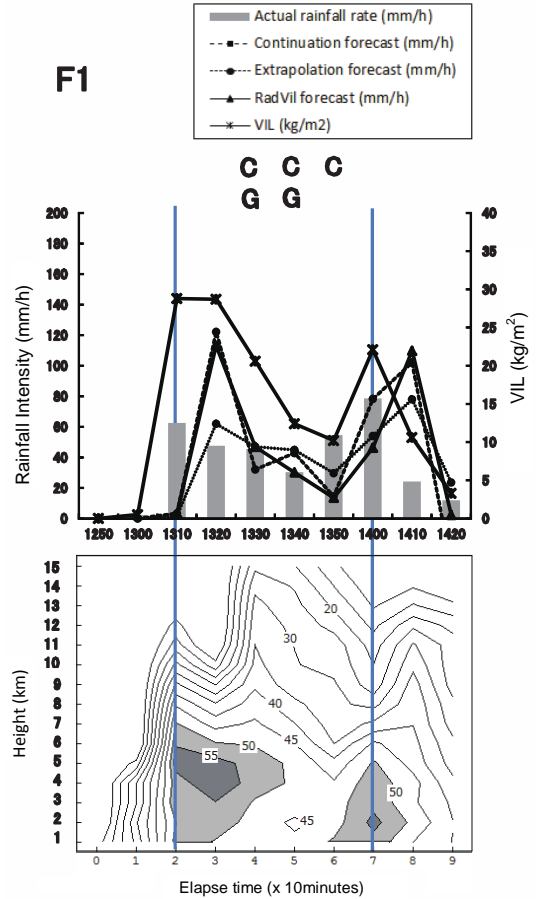


Fig. 12. Same as Fig. 5 for convective cell F1.

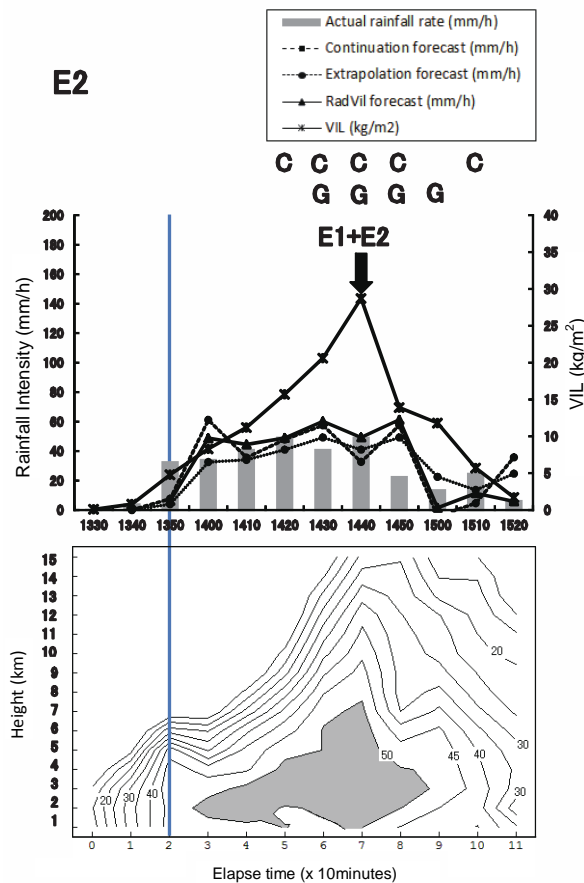


Fig. 11. Same as Fig. 5 for convective cell E2.

In the case of C3 (Fig. 6), a rainfall peak occurred only 10 minutes after separation from C1. The effect of the nowcasting rainfall peak could not be seen in the forecasting methods based on radar observation (core aloft, VIL, echo-top height). Regarding lightning, C occurred from 10 minutes before the rainfall peak. Calculations for extrapolation and RadVil forecasts could not be started before the rainfall peak.

D1 (Fig. 7) had two rainfall peaks. Ten minutes before the first rainfall peak, a core of 51 dBZ appeared at the 2 km level and VIL showed a tendency to increase. The second rainfall peak appeared at the same time as when a core was detected at the 5 km level. The echo-top height increased rapidly 20 to 30 minutes before the second peak. C lightning was observed at 30 minutes before the first rainfall peak, but C and G were not detected until the second rainfall peak. Continuation and RadVil forecasts showed a false peak 10 minutes before the actual rainfall peak.

A core aloft greater than 50 dBZ had existed in D2 (Fig. 8) at the 2-5 km level from 50 minutes before the appearance of a rainfall peak. A VIL peak also appeared 30 minutes before the rainfall peak. C and G lightning were observed from 20 minutes before the rainfall peak. Values of the three quantitative forecasts were valid until 10 minutes before the rainfall peak, but underestimated

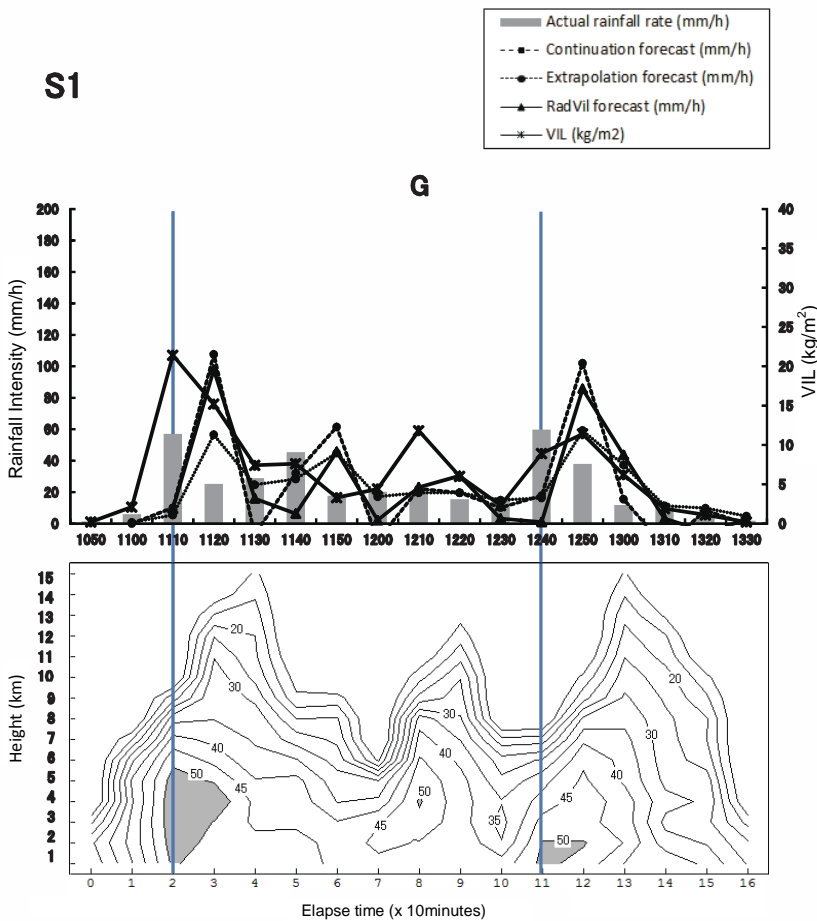


Fig. 13. Same as Fig. 5 for convective cell S1.

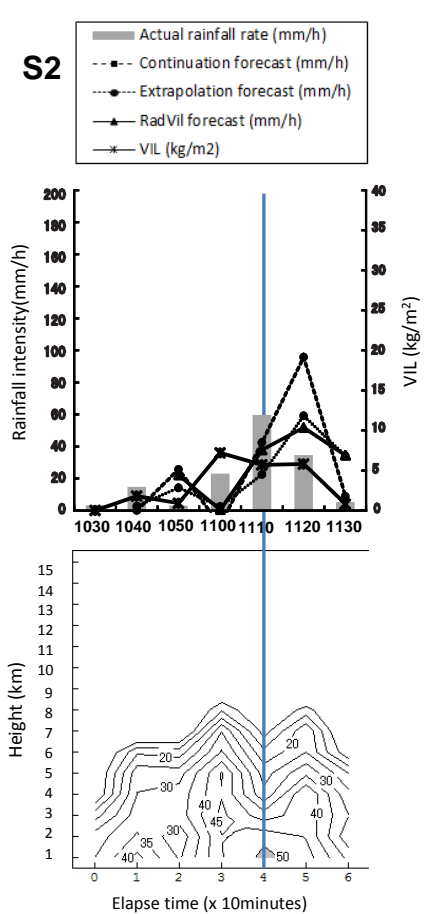


Fig. 14. Same as Fig. 5 for convective cell S2.

the rainfall peak.

The horizontal scale of D3 was the smallest of the 8 heavy rainfall cells, and caused only the total rainfall amount of 29 mm during one hour. A core of 54 dBZ appeared in D3 (Fig. 9) at the 3 km level 10 minutes before the rainfall peak. The echo-top height increased rapidly 10-20 minutes before the rainfall peak. RadVil forecasts gave good rainfall peak values, but immediately after the peak, overestimated the rainfall intensity the same as in the other cases.

E1 and E2 (Figs. 10 and 11) were generated separately and merged into a larger convective cell at 1440 JST. A core of 54 dBZ appeared 10 minutes before the rainfall peak of E1 at the 2 km level (Fig. 10). VIL was increasing 20 minutes before the rainfall peak and there was also a VIL peak at the time of merging with E2. The three forecast values underestimated the values of the rainfall peak in E1. E2 had a peak at 1350 JST with a rainfall intensity of less than that of criteria (Fig. 11). No forecast method was effective in E2. On the other hand, E2 showed a prominent increase in VIL before merging with E1 as well as in the case of E1, and such a tendency should be examined as a precursor of cell merging.

F1 had two rainfall peaks (Fig. 12). No method forecasted the first peak except for the rapid increase in echo-top height. C and G lightning occurred 30 minutes before the second rainfall peak. The three forecast methods

showed relatively good values before the second peak.

S1 was generated and disappeared alone with a long lifetime of 160 minutes. S2 was the smallest in horizontal size and the shortest in lifetime among the 10 convective cells. One of the differences from the 8 heavy rainfall convective cells was that S1 and S2 were relatively shallow except for three echo-top peaks of E1 (Figs. 13 and 14). Echo-top height showed a rapidly increase before the first peak of S1. A core of 46 dBZ appeared at a height of 3 km 10 minutes before the rainfall peak of S2.

5. Discussion

The effectiveness of 4 qualitative forecasting methods and 3 quantitative methods were examined in 8 heavy rainfall convective cells. They involved a total of 10 rainfall peaks. Results are summarized as follows:

- Core aloft: Radar observations, e.g., Chisholm and Renick (1972) [28] or Fig. 2.1 of Burgess and Lemon (1990) [29] and numerical models, e.g., Fig. 10 of Ferrier and House (1989) [30], show a scenario in which a precipitation core is formed in the middle-lower troposphere in thunderstorms and caused rainfall after a descent toward the surface. Cores greater than 50 dBZ appeared before 6 out of 10 rainfall

peaks. This situation was prominent in C1. Four cores in these, however, appeared only 10 minutes before rainfall peaks. Also, in three cases, the initiation height of cores was only 2 km. Further evaluation will be required for the cores aloft method as a precursor of forecasting rainfall peaks.

- VIL: VIL showed a rapid increase before 4 of 10 rainfall peaks. VIL peaks, however, appeared at the same time as the rainfall peaks in 5 cases. This result corresponds to the results of Sato et al. (2009) [15]; they examined the total of 750 thunderstorms generated in various places in Japan and found that the cross-correlation coefficient between time-series of rainfall intensity near the surface and that of VIL showed a maximum in cases in which lag time was zero. VIL is an effective parameter in tracking convective cells because it contains rainfall information in the vertical direction, but more validation will be required before using it as a forecasting parameter of rainfall peak.
- Echo-top height: There was a trend in rapidly increased echo-top height 10 to 20 minutes before 4 rainfall peaks of 10. Since the 1980s, the JMA has used echo-top height data as one of the parameters for monitoring deep convective clouds that may cause heavy rainfall. The result of this study partially support the validity of the empirical method to monitor heavy rainfall.
- Lightning activity: C or G or both types of lightning were detected 10-30 minutes before 5 rainfall peaks of 10. Fig. 4 of Williams et al. (1989) [31] showed that intracloud lightning (C in this paper) occurred from 4 minutes before a rainfall peak in a single-cell thunderstorm generated in Florida, U.S. Little research has been made in Japan on rainfall nowcasting methods using lightning discharge. In the present research, some cases were effective and other cases were not in nowcasting. Since the presence or absence of lightning discharge depends on atmospheric stratification and convection activity, there are cases of heavy rainfall without lightning activity. Lightning discharge was not detected, for instance, before and after heavy rainfall in the case of thunderstorms that caused local heavy rainfall of 107 mm/h in Itabashi, Tokyo, on July 5, 2010 [32]. In Yamada's case, the height of thunderstorms was about 10 km, which does not meet the condition for lightning generation discussed thus far, e.g., -20° in a region with a reflectivity of 30 dBZ [33] or -10° in a region with a reflectivity of 40 dBZ [34].
- Three quantitative forecast methods: One or two of the three quantitative forecasting methods were effective in 4 of 10 rainfall peaks. Only three cases, however, satisfied adequate accuracy, which suggests the difficulty in quantitative nowcasting of rain intensity using existing observation data. The larger

the rainfall intensity thunderstorms brought about, the more error occurred in quantitative forecasting. RadVil and extrapolation methods often indicated false peaks at 10 minutes after actual rainfall peaks as a result of their inherent feature, and that also makes it difficult to designate peak time of rainfall appropriately.

6. Conclusions

Heavy local rainfall occurred due to thunderstorms generated over Zoshigaya, Tokyo, on August 5, 2008. A feasibility study of very short-term forecasts (nowcast) of rainfall was made targeting air-mass thunderstorms generated in areas for which heavy rainfall warnings were issued by the JMA on this day. Three-dimensional data obtained from JMA radar operation and data from the JMA lightning detection system LIDEN were used. Four qualitative forecast methods – cores aloft, VIL, echo-top height, and lightning activity – and three quantitative forecasting methods – continuation, extrapolation and RadVil – were examined to forecast time and rainfall intensity at rainfall peaks.

The most effective of the 4 qualitative methods is thought to be core aloft, and should be surveyed using much more samples of thunderstorms. The other 3 qualitative methods are not in a stage of operational use. The three quantitative forecast methods have low ability to identify rainfall peaks from thunderstorms. Although the RadVil method explicitly contains a process of formation of rain water in thunderstorms, it had no advantage over the continuation method or the extrapolation method.

Causes that make nowcasting of heavy rainfall difficult in this study and issues in the future are summarized as follows:

- The time resolution of data used in this study – 10 minutes – was insufficient to track time change in feature of thunderstorms. In some convective cells, a core was seen to suddenly appear aloft and then disappear without reaching the surface. Higher time-resolution data are also required in VIL and RadVil analyses. The effects of the forecast methods discussed in this study should be evaluated once again using three-dimensional radar data with shorter – hopefully 1-2 minute – time intervals in accordance with rapid changes in the internal structure of thunderstorms.
- The method of Stalker and Knupp (2002) [35], which calculates vertical flow inside thunderstorms using the Doppler velocity of multiple radars, is worthy of discussion because it gives us information on cloud dynamics inside thunderstorms.
- More understanding of processes of multi-cell process and merging of convective cells is required. As seen for convective cell C1, the merging of convective cells induces a high possibility of causing

heavy rainfall. New convective cells were occasionally generated nearby an existing convective cell and caused heavy rainfall soon after merging with the old cell.

- Development of automatic three-dimensional core tracking technique such as Fukamachi et al. (2008) [36] are greatly required for extending research on the evolution of thunderstorm more efficiently and more practically.
- High time-resolution satellite observation as 1-2 minute interval, as shown in the MTSAT trial operation from 2010 [37], is expected to be an effective tool for monitoring initial and growing stages of thunderstorms in which cloud droplets and ice crystals, rather than rain droplets, are dominant.
- Comprehensive understanding of thunderstorms will be given by new observation technology such as high-speed scanning radars [38], dual polarization radars, high-density surface and GPS observation networks, as well as cloud-resolving numerical models with 4-dimensional data assimilation [39]. The research project "Tokyo Metropolitan Area Convection Study for Extreme Weather Resilient Cities 2000-2004" [40, 41] will give us a chance to improve understanding concerning thunderstorms and relating local heavy rainfall.

Acknowledgements

3-D radar and LIDEN data used in this study were provided by the Observations Department of the JMA. Mr. Hiroshi Miyagi of the Forecast Department of the JMA offered detailed information on the data. Mr. Toshihiro Sato of the Observations Department and Mr. Shogo Edamoto (now at the Wakayama meteorological observatory) developed the program for semi-automatically tracking convective cells and extracting three-dimensional data in specific regions from archive data. Dr. Fumiaki Fujibe of the Meteorological Research Institute of the JMA, Dr. Kosaku Moteki of the Japan Agency for Marine-Earth Science Technology and two peer reviewers provided the author with much valuable advice. The author wishes to thank all for their invaluable assistance.

This study was made in the research project "Tokyo Metropolitan Area Convection Study for Extreme Weather Resilient Cities 2000-2004" supported by Strategic Funds for the Promotion of Science and Technology of the Japanese Ministry of Education, Culture, Sports, Science and Technology.

References:

- [1] M. Ishihara, "Radar echo population of air-mass thunderstorms and nowcasting of thunderstorm-induced local heavy rainfalls Part 1: statistical characteristics," *J. Disaster Research*, Vol.8, No.1, pp. 57-68, 2013 (this number).
- [2] A. Okubo, N. Mashiko, N. Sakamaki, M. Nishi, E. Nagata, and T. Takami, "Prediction of convective rain at warm phase in Tokyo area based on the strong rain scenario - Improvement for securing at the "lead time" in issuing warnings and advisories for heavy rain," *J. Meteor. Research*, Japan Meteorological Agency, Vol.59, pp. 41-55, 2007 (in Japanese).
- [3] Y. Makihara, "Steps towards decreasing heavy rain disaster by short-range precipitation and land-slide forecast using weather radar accompanied by improvement of meteorological operational activities," *Tenki*, Vol.54, pp. 21-33, 2007 (in Japanese).
- [4] I. Sugiura, M. Kunitsugu, Y. Tsujimura, and T. Makihara, "Outline on the JMA precipitation nowcasting system," 2005 Spring Meeting of the Meteorological Society of Japan, C463, pp. 208, 2005.
- [5] V. Lakshmanan, T. Smith, G. Stumpf, and K. Hondl, "The warning decision support system Integrated information," *Wea. Forecasting*, Vol.22, pp. 596-612, 2007.
- [6] M. Dixon and G. Wiener, "TITAN: Thunderstorm identification, tracking, analysis, and nowcasting - A radar-based methodology," *J. Atmos. Ocean. Technol.*, Vol.10, pp. 785-797, 1993.
- [7] B. W. Golding, "Nimrod: A system for generating automated very-short-range forecasts," *Meteor. Appl.*, Vol.5, pp. 1-16, 1998.
- [8] C. E. Pierce, P. J. Hardaker, C. G. Collier, and C. M. Haggett, "GANDOLF: A system for generating automated nowcasts of convective precipitation," *Meteor. Appl.*, Vol.7, pp. 341-360, 2000.
- [9] S. Lapczak, E. Aldcroft, M. Stanley-Jones, J. Scott, P. Joe, P. Van Rijn, M. Falla, A. Gagne, P. Ford, K. Reynolds, and D. Hudak, "The Canadian National Radar Project," Preprints, 29th Int. Conf. on Radar Meteorology, Montreal, Canada, Amer. Meteor. Soc., pp. 327-330, 1999.
- [10] H.-J. Koppert, T. S. Pederson, B. Zurcher, and P. Joe, "How to make an international meteorological workstation project successful," Preprints, 20th Int. Conf. on Interactive Information and Processing Systems (IIPS) for Meteorology, Oceanography, and Hydrology, Seattle, WA, Amer. Meteor. Soc. IL.1, 2004.
- [11] C. E. Pierce, E. Ebert, A. W. Seed, M. Sleigh, C. G. Collier, N. I. Fox, N. Donaldson, J. W. Wilson, R. Roberts, and C. K. Mueller, "The nowcasting of precipitation during Sydney 2000: An appraisal of the QPF algorithms," *Wea. Forecasting*, Vol.19, pp. 7-21, 2004.
- [12] P. Joe, D. Burgess, R. Potts, T. Keenan, G. Stumpf, and A. Treloar, "The S2K severe weather detection algorithms and their performance," *Wea. Forecasting*, Vol.19, pp. 43-69, 2004.
- [13] J. W. Wilson, Y. Feng, M. Chen, and R. D. Roberts, "Nowcasting challenges during the Beijing Olympics: Successes, failures, and implications for future nowcasting systems," *Wea. Forecasting*, Vol.25, pp. 1691-1714, 2010.
- [14] Observations Department, JMA, "Newly developed radar observation system and their radar information," *Weather Service Bulletin*, Japan Meteorological Agency, Vol.74, pp. 38-42, 2007 (in Japanese).
- [15] T. Sato, K. Tsuda, K. Shibata, M. Yasuda, T. Abe, K. Sugawara, and H. Aragaki, "Characteristics of radar echo indices concerning precipitation cells," *Weather Service Bulletin*, Japan Meteorological Agency, Vol.76, pp. 64-72, 2009 (in Japanese).
- [16] Japan Meteorological Agency, "Knowledge on weather, forecast terms, precipitation," the JMA web site, http://www.jma.go.jp/jma/kishou/now/yougo_hp/kousui.html [accessed on January 22, 2013]
- [17] D. R. Greene and R. A. Clark, "Vertically integrated liquid water - A new analysis tool," *Mon. Wea. Rev.*, Vol.100, pp. 548-552, 1972.
- [18] H. Inoue and T. Inoue, "Characteristics of the water-vapor field over the Kanto district associated with summer thunderstorm activities," *SOLA*, Vol.3, pp. 101-104, 2007.
- [19] J. S. Marshall and W. M. Palmer, "The distribution of raindrops with size," *J. Meteor.*, Vol.5, pp. 165-166, 1948.
- [20] J. S. Marshall, W. Hirschfeld and K. L. S. Gunn, "Advanced in radar weather," *Advances in Geophysics*, Vol.2, pp. 1-56, 1955.
- [21] Observations Department, JMA, "Introduction to the JMA lightning detection system LIDEN," *Kishou*, Vol.45, pp. 17426-17429, 2001 (in Japanese).
- [22] T. Takahashi, "Thunderstorm electrification - A numerical study," *J. Atmos. Sci.* Vol.41, pp. 2541-2558, 1984.
- [23] B. Boudevillain, H. Andrieu, and N. Chaumerliac, "Evaluation of RadVil, a radar-based very short-term rainfall forecasting model," *J. Hydrometeor.*, Vol.7, pp. 178-189, 2006.
- [24] N. Mura, "A case study on a local heavy rainfall occurred in Tokyo on August 5, 2008 and its numerical simulation using the JMA-NHM model," *Tenki*, Vol.56, pp. 933-938, 2009 (in Japanese).
- [25] A. Kato and M. Maki, "Localized heavy rainfall near Zoshigaya, Tokyo, Japan on 5 August 2008 observed by X-band polarimetric radar - Preliminary analysis -," *SOLA*, Vol.5, pp. 89-92, 2009.
- [26] D. -S. Kim, M. Maki, S. Shimizu, and D. -I. Lee, "X-band dual-polarization radar observations of precipitation core development and structure in multi-cellular storm over Zoshigaya, Japan, on August 5, 2008," *J. Meteor. Soc. Japan*, Vol.90, pp. 701-719, 2012.
- [27] Bureau of Sewerage, Tokyo Metropolitan Government, "Report on the accident of the reconstruction of the Zoshigaya sewerage main line," 12p, 2008.
- [28] A. J. Chisholm and J. H. Renick, "The kinematics of multicell and supercell Alberta hailstorms," *Alberta Hail Studies*, 1972, Research Council of Alberta Hail Studies Rep. No.72-2, pp. 24-31, 1972.
- [29] D. W. Burgess and L. R. Lemon, "Severe thunderstorm detection by radar," *Radar in Meteorology* (edited by D. Atlas), Amer. Meteor. Soc. pp. 619-647, 1990.

[30] B. S. Ferrier and R. A. Houze, "One-dimensional time-dependent modeling of GATE cumulonimbus convection," J. Atmos. Sci., Vol.46, pp. 330-352, 1989.

[31] Williams, E. R., M. E. Weber, and R. E. Orville, "The relationship between lightning type and convective state of thunderclouds," J. Geophys. Res., Vol.94, pp. 13213-13220, 1989.

[32] Y. Yamada, "Structure of a thunderstorm causing heavy rainfall in Itabashi, Tokyo on July 5, 201," 2010 Autumn Meeting of the Meteorological Society of Japan, C354, pp. 244, 2010 (in Japanese).

[33] K. Michimoto, "A study of radar echoes and their relation to lightning discharge of thunderclouds in the Hokuriku District. Part I: Observation and analysis of thunderclouds in summer and winter," J. Meteor. Soc. Japan, Vol.69, pp. 327-336, 1991.

[34] M. S. Gremillion and R. E. Orville, "Thunderstorm characteristics of cloud-to-ground lightning at the Kennedy Space Center, Florida: A study of lightning initiation signatures as indicated by the WSR-88D," Wea. Forecasting, Vol.14, pp. 640-649, 1999.

[35] J. R. Stalker and K. R. Knupp, "A method to identify convective cells within multicell thunderstorms from multiple Doppler radar data," Mon. Wea. Rev., Vol.130, pp. 188-195, 2002.

[36] Y. Fukamachi, T. Shinoda, H. Uyeda, and K. Tsuboki, "Development of a three-dimensional detection algorithm for precipitation cells," Proceeding, 2008 Autumn Meeting of the Meteorological Society of Japan, P171, pp. 418, 2008.

[37] I. Okabe, Y. Izumikawa, and T. Imai, "On the development of a product for detecting rapidly developing cumuli," 2008 Spring Meeting of the Meteorological Society of Japan, C456, pp. 217, 2011.

[38] E. Yoshikawa, T. Ushio, Z. Kawasaki, and V. Chandrasekar, "Dual-directional radar observation for preliminary assessment of the Ku-band broadband radar network," J. Atmos. Ocean Technol., Vol.29, pp. 1757-1767, 2012.

[39] T. Kawabata, T. Kuroda, H. Seko, and K. Saito, "A cloud-resolving 4D VAR assimilation experiment for a local heavy rainfall event in the Tokyo metropolitan area," Mon. Wea. Rev., Vol.139, pp. 1911-1931, 2011.

[40] M. Ishihara, T. Kobayashi, and O. Suzuki, "A field campaign project for study of thunderstorm-induced heavy local rainstorms in the Tokyo Metropolitan Area," 2011 Japan Geoscience Union Meeting, U022-02, 2011.

[41] M. Maki and Co-authors, "Social experiments on extreme weather resilient cities," 2011 Japan Geoscience Union Meeting, U022-01, 2011.

vector is obtained using cross-correlation methods from rainfall distribution in successive time steps. In our study, the movement of each convective cell was tracked subjectively. S is determined using Eq. (1) as follows:

$$S(t) = \frac{VIL(t) - VIL^*(t - \Delta t)}{\Delta t} + P(t) \dots (3)$$

An asterisk (*) indicates the advection of the field of $VIL(t - \Delta t)$ within time Δt . $\tau(t)$ is obtained using Eq. (2).

Convective systems are supposed to be in a steady state in forecasting time (10 minutes in this paper) with fixing advection speed, S and t in this period. The following is obtained when Eq. (2) is substituted in Eq. (1):

$$\frac{d(VIL)}{dt} + \frac{VIL(t)}{\tau(t)} = S(t) \dots (4)$$

This first-order nonhomogeneous ordinary differential equation is solved analytically using the method of variation of constants. A forecasting equation for VIL is obtained as follows:

$$VIL(t + dt) = VIL^*(t)e^{-\frac{dt}{\tau}} + S\tau(t)(1 - e^{-\frac{dt}{\tau}}) \dots (5)$$

Forecast values of P are determined using Eq. (2) from VIL obtained by Eq. (5). Eq. (5) corresponds to Eq. (8) in the paper of Boudevillain et al. (2006) as shown below, but their expression of Eq. (8) is thought to be a misprint.

$$VIL(t + dt) = VIL^*(t)e^{\frac{dt}{\tau}} - S\tau(t)(1 - e^{\frac{dt}{\tau}}) \dots (6)$$

Appendix A. Rainfall Forecasting Model RadVil Formulated by Boudevillain et al. (2006) [23]

RadVil is a rainfall forecasting model that considers the balance of rain water in convection. Both rainfall intensity at the surface and VIL , which is rain water integrated in an air column, are quantities obtained from three-dimensional radar data. Time change in VIL is expressed as follows:

$$\frac{d(VIL)}{dt} = S(t) - P(t) \dots (1)$$

S indicates the rate of rain water generation in an air column, consisting of vapor condensation, conversion from cloud water to rain water, and melting. P is rainfall intensity ($\text{kgm}^{-2}\text{s}^{-1}$) at the surface, the output rate of rain water from an air column.

$$P(t) = \frac{VIL(t)}{\tau(t)} \dots (2)$$

$\tau(t)$ is termed reaction time. This parameter has a time scale indicating the conversion efficiency of rain water in an air column (VIL) to rainfall on the surface. Each horizontal radar grid is defined as an air column.

RadVil calculates rainfall intensity and VIL from three-dimensional radar data at each time step. An advection